



COBEM2021-1683

CHARACTERIZATION OF THE THERMO-HYDRAULIC PERFORMANCE OF A $\text{La}(\text{Fe},\text{Mn},\text{Si})_{13}\text{H}_y$ REGENERATOR

Hígor Feltrin Teza

higor.teza@polo.ufsc.br

Bernardo Peressoni Vieira

bernardo.vieira@polo.ufsc.br

Natália Maleski de Sá

natalia.sa@polo.ufsc.br

Alan Tihiro Dias Nakashima

alan.nakashima@polo.ufsc.br

Guilherme Fidelis Peixer

guilherme.peixer@polo.ufsc.br

Gislaine Hoffmann

gislaine@polo.ufsc.br

Jaime Andrés Lozano

jaime@polo.ufsc.br

Jader Riso Barbosa Jr

jrb@polo.ufsc.br

Polo - Research Laboratories for Emerging Technologies in Cooling and Thermophysics, Department of Mechanical Engineering Federal University of Santa Catarina, Florianópolis, SC, 88040-900, Brazil

Abstract. *Magnetic refrigeration is one of the most promising caloric cooling technologies regarding theoretical energy efficiency and reduction of the impact on the environment. Therefore, improving the components of a magnetocaloric refrigeration device in order to make it commercially viable is essential. One of the main components is the active magnetic regenerator (AMR), which is filled with a magnetocaloric material responsible for the refrigerant effect. A proper regenerator design must consider its heat exchange capacity and the restriction it imposes on the mass flow rate provided by the pump, what can be evaluated by performing a thermo-hydraulic characterization in order to obtain its effectiveness and friction factor. Therefore, this work performed a characterization of a packed spheres bed regenerator, composed of particles with an average diameter of 0.75 mm, a porosity of approximately 38%, and 10 layers of a $\text{La}(\text{Fe},\text{Si},\text{Mn})_{13}\text{H}_y$ alloy, which is a magnetocaloric material. Besides the thermo-hydraulic characterization, it is fundamental to assess the stability of the material due to the brittleness commonly presented by these alloys. Therefore, the pressure drop tests are performed regularly to monitor any increase, which would mean the regenerator is breaking apart. All the experimental conditions presented high effectiveness, i.e., above 95% and the regenerator doesn't shows significant pressure drop increases, indicating that it is mechanically stable. The pressure drop tests results were compared to the Ergun's equation and shape factors were used to calibrate the numerical model to the regenerator porous medium.*

Keywords: *magnetic refrigeration, La-Fe-Si alloy, active magnetic regenerator, effectiveness, pressure drop.*

1. INTRODUCTION

Nowadays, refrigeration and air conditioning devices are responsible for about 17 % of global electricity consumption, and the demand for these devices is rapidly increasing (Kitanovski, 2020). For that reason, the development of more energy efficient systems has been one of the main objectives of this area. To achieve this goal, one of the most promising technologies is magnetocaloric refrigeration, which is able to theoretically achieve higher efficiencies when compared with vapor compression systems due to its nearly isentropic magnetization and demagnetization processes (Kitanovski *et al.*, 2015). Besides the potential for more energy efficient systems, there are other advantages to this technology. The use of solid-state refrigerants prevents leakages, in contrast with the utilization of refrigerant fluids in the vapor compression technology, which often comes with undesirable properties such as flammability (R600a), toxicity (R717) or high GWP.

One of the main components of a magnetic refrigerator is the Active Magnetic Regenerator (AMR), which is a porous medium composed (often with several layers) of a magnetocaloric material (MCM), i.e., a material that presents the magnetocaloric effect (MCE). Therefore, when the MCM undergoes magnetization under adiabatic conditions, its temperature increases while under demagnetization there is a reduction in temperature. This can be explained by the magnetic and

lattice entropy variation. During an adiabatic and reversible (i.e. isentropic) process, the total entropy change, which can be approximately described as the sum of the magnetic and lattice contributions, is equal to zero. Thereby, the reduction of magnetic entropy by magnetization induces an increase in the entropy of lattice, i.e, an increase in temperature, and the opposite occurs in demagnetization (Smith *et al.*, 2012). With these properties, the MCM can be used to perform a refrigeration cycle.

The refrigeration cycle is based in the idealized Brayton thermo-magnetic cycle, which is composed of two isofield and two isentropic processes (Rowe *et al.*, 2015; Trevizoli and Barbosa, 2020) in which the AMR acts both as a refrigerant and a heat storage medium. First, there is an adiabatic magnetization of the porous medium, resulting in the increase of the AMR temperature through the MCE. Afterwards, the fluid flows from the cold to the hot reservoir, crossing the matrix, absorbing heat, and thus cooling it. In this step, the fluid exits at the hot reservoir and rejects the heat absorbed from the matrix. In the next step, the solid matrix undergoes an adiabatic demagnetization, in which its temperature decreases. After that, the fluid flows from the hot to the cold reservoir at constant field, rejecting heat to the matrix. In this process, the fluid temperature decreases, which allows the fluid to exit the regenerator below the cold reservoir temperature. Therefore, it has the potential to absorb heat from the cold reservoir. In an AMR, each volume of the matrix performs an individual cycle, that, when combined, form a single Brayton refrigeration cycle.

Thus, the heat transfer between the fluid and the porous matrix is a critical part of the cycle in such a way that along with the viscous dissipation, imperfect heat transfer is one of the main sources of irreversibilities inside AMRs (Lei *et al.*, 2018), thereby, the heat transfer performance must be as high as possible to reduce these irreversibilities. For this reason, it is essential to characterize the heat transfer performance of the AMR. In order to do so, it is important to carry out the tests in a way that separates the heat transfer performance from the effects of MCE during the operation, which can be achieved by performing the experiments without the application of a magnetic field in the regenerator.

In addition to the heat transfer tests, it is important to carry out pressure drop tests in the matrix since the viscous dissipation is one of the major mechanisms of entropy generation in the AMR, as mentioned above. Besides, it is important to check the integrity of the regenerator through its pressure drop, which tends to increase when there is mechanical failure throughout the tests. This happens mainly due to the brittleness commonly found in LaFeSi alloys (Lionte *et al.*, 2021).

2. EXPERIMENTAL APPARATUS

Figure 1 shows the experimental apparatus, which is composed of a stationary regenerator bed, two brazed heat exchangers, one gear pump, four solenoid valves, two mass flow meters, six thermocouples, six pressure transducers and two water baths (not shown in the figure). The sensors and transducers details are shown in Tab. 1.

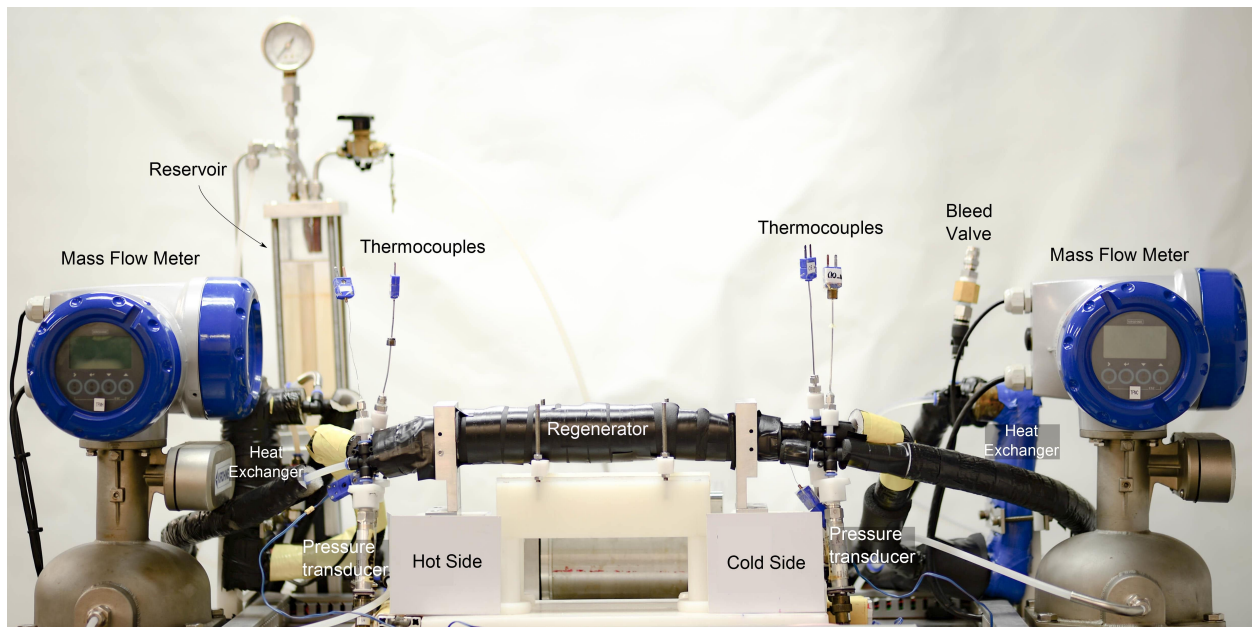


Figure 1: Experimental apparatus used in the thermo-hydraulic characterization of the AMR

It is important to mention that the heat exchangers are responsible for emulating an ideal heat exchanger between the fluid and the heat sink and source. Therefore, it is possible to set the temperature span at which the regenerator is operating by setting the temperature of the two thermal baths. The thermocouples are used to evaluate the temperatures at which the fluid enters and exits the regenerator and the pressure transducers are responsible for measuring the pressure drop across the regenerator. The oscillatory flow is guaranteed by the solenoid valves, which can be classified as high and

Table 1: Instrumentation of the experimental apparatus

Sensor/Transducer	Quantity	Company	Model	Uncertainty
Mass Flow Meter	2	Krohne	Optimass 3300C-S04	$\pm 1 \%$
Thermocouple	6	Omega	SCPSS-020G-6	0.2 K
Pressure	5	Omega	PX613-200G5V	± 0.5 kPa
Pressure	1	Omega	PX613-300G5V	± 0.8 kPa

low pressure valves (respectively HPV and LPV) in a way that for the cold-to-hot side blow (cold blow), two valves are open (one of the HPV and the other of the LPV) so the fluid can flow only in one direction. For the hot-to-cold side blow (hot blow), the other pair of valves are open. A schematic diagram of the apparatus can be found in Fig. 2.

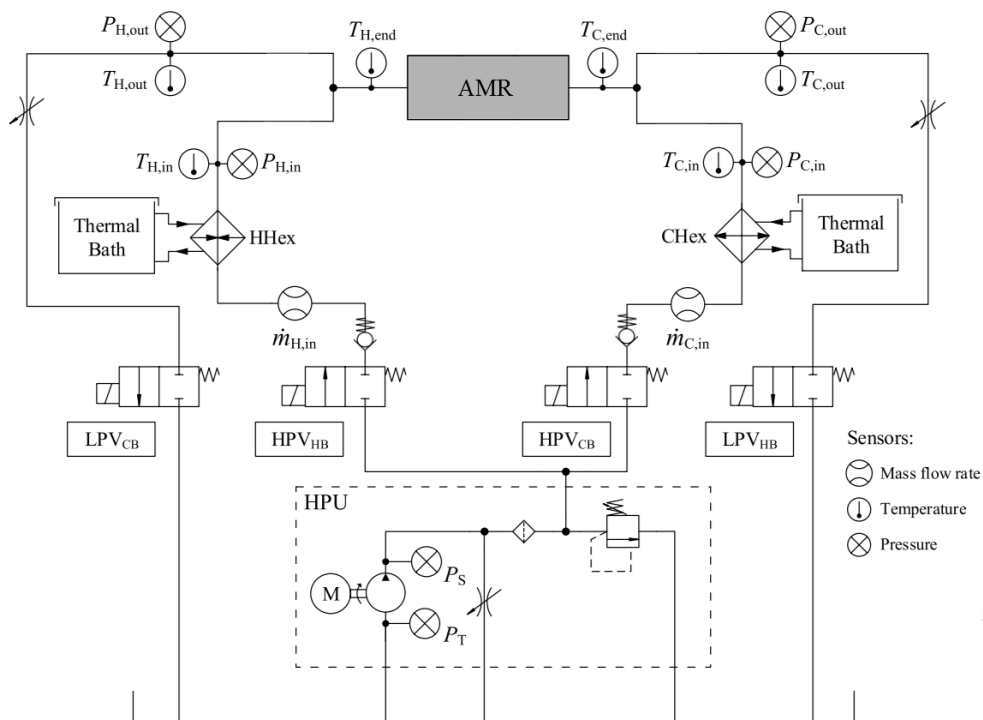


Figure 2: Schematic diagram of the experimental apparatus. Adapted from Vieira *et al.* (2021)

In order to carry out the tests, the regenerator was assembled into a packed spheres bed composed of 10 layers of Calorivac-HS, i.e., a $\text{La}(\text{Fe},\text{Si},\text{Mn})_{13}\text{H}_y$ alloy provided by Vacuumschmelze. The details of the regenerator are shown in the Tab. 2 below and a schematic representation of the 10 layers regenerator is shown in Fig. 3, which shows the layering of materials with different Curie temperatures along the regenerator according to the position of the hot and cold reservoirs. The circles inside each layer represent the particles of MMC (out of scale), which are also shown in real scale in Fig. 6.

Table 2: Regenerator's details

Dimension/Property	Value
Internal diameter	24.2 mm
Available length ⁽¹⁾	114 mm
MCM mass	233.5 g
Particle diameter ⁽²⁾	0.755 mm
Porosity	37.9 %

⁽¹⁾ Considering the frames to separate the layers and the end parts

⁽²⁾ The average of the particle diameter distribution

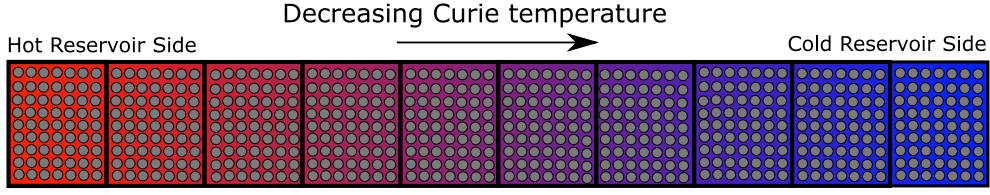


Figure 3: Schematic representation of the 10 layers regenerator.

3. EXPERIMENTAL METHOD

The experimental method applied to the effectiveness and pressure drop measurements will be presented in this section.

3.1 EFFECTIVENESS MEASUREMENTS

In order to characterize the regenerator regarding its heat exchange performance, a method of evaluation needs to be selected in order to allow its performance to be quantified and compared to others. One of the consistently used methods in this case is the effectiveness (ϵ) - NTU method.

This method is widely utilized because: (i) The effectiveness provides the criterion for evaluating the heat transfer and can be derived direct from temperature measurements when assuming balanced flow conditions, i.e, the thermal capacity rates at both directions are the same, and (ii) The NTU (number of transfer units) provides a "measure" of the thermal size of the regenerator (Liang *et al.*, 2020). For that reason, in this work, the regenerator heat transfer performance is characterized in terms of effectiveness and NTU, in which the effectiveness is defined in Eq. (1):

$$\epsilon = \frac{\dot{Q}_{\text{blow}}}{\dot{Q}_{\text{max}}}, \quad (1)$$

where \dot{Q}_{blow} is the actual transferred heat in the heat exchanger (in this case the regenerator) and \dot{Q}_{max} is the maximum heat exchange possible in the regenerator. Therefore, the effectiveness for each blow can be written as:

$$\epsilon_{\text{cb}} = \frac{\dot{m}_{\text{cb}}c_p(\bar{T}_{\text{H,out}} - T_{\text{C,in}})}{(\dot{m}c_p)_{\text{min}}(T_{\text{H,in}} - T_{\text{C,in}})} \quad (2)$$

$$\epsilon_{\text{hb}} = \frac{\dot{m}_{\text{hb}}c_p(T_{\text{H,in}} - \bar{T}_{\text{C,out}})}{(\dot{m}c_p)_{\text{min}}(\bar{T}_{\text{H,in}} - T_{\text{C,in}})} \quad (3)$$

where the product $\dot{m}c_p$ is the thermal capacity rate and the subscripts cb and hb are for cold blow (when fluid flows through the regenerator from the cold reservoir to the hot one) and hot blow (when fluid flows through the regenerator from the hot reservoir to the cold one), respectively. $(\dot{m}c_p)_{\text{min}}$ is the smaller of the two thermal capacity rates between the cold blow and the hot blow. $T_{\text{H,in}}$ and $T_{\text{C,in}}$ are the regenerator inlet fluid temperatures during the hot blow (therefore the hot thermal reservoir temperature) and during the cold blow (therefore the cold reservoir temperature), respectively, and $\bar{T}_{\text{H,out}}$ and $\bar{T}_{\text{C,out}}$ are the average outlet temperature of the fluid in the cold blow and hot blow, respectively.

Under balanced flow conditions, the effectiveness can be simplified as a function of only the temperatures as shown in Eq. (4) and Eq. (5).

$$\epsilon_{\text{cb}} = \frac{\bar{T}_{\text{H,out}} - T_{\text{C,in}}}{T_{\text{H,in}} - T_{\text{C,in}}} \quad (4)$$

$$\epsilon_{\text{hb}} = \frac{T_{\text{H,in}} - \bar{T}_{\text{C,out}}}{\bar{T}_{\text{H,in}} - T_{\text{C,in}}} \quad (5)$$

The NTU is a non dimensional parameter defined as shown in the Eq. (6) below:

$$NTU = \frac{hA_{\text{ht}}}{\dot{m}c_p} \quad (6)$$

where h is the interstitial heat transfer coefficient and A_{ht} is heat transfer surface area. To obtain the interstitial heat transfer coefficient, the correlation proposed by Pallares and Grau (2010) was used including a degradation factor (Hausen, 1983; Engelbrecht, 2008) to consider the temperature gradients that occur within the regenerator material, while the heat transfer surface area is estimated by (Kaviany, 1995; Vieira *et al.*, 2021):

$$A_{\text{ht}} = V_{\text{reg}}\beta \quad (7)$$

$$\beta = (1 - \epsilon) \frac{6}{d_p} \quad (8)$$

where β , ϵ , V_{reg} and d_p are, respectively, the surface area density, the regenerator's porosity, its volume and the particle diameter.

In a regenerator, increasing the NTU results in a higher effectiveness, i.e., higher heat transfer between the fluid and the solid matrix, which will result in a higher overall efficiency of the AMR in the thermodynamic cycle it performs (Trevizoli and Barbosa, 2020).

Another important non dimensional parameter is the utilization factor (ϕ), which is defined as the ratio between the total heat capacity of the fluid that flows through the matrix in one blow and the total heat capacity of the solid matrix (Eq. 9). Thus, having a high matrix heat capacity allows the regenerator to absorb large amounts of heat without changing its temperature (Nellis and Klein, 2009), which results in a regenerator with a higher effectiveness.

$$\phi = \frac{\dot{m}_f c_{p,f} \tau}{m_s c_{p,s}} \quad (9)$$

In the equation above, the subscripts "f" and "s" refer to the fluid and solid (MCM) phases and τ is the blow time period, which is given by the frequency (f) and the blow fraction (ψ), which represents the ratio between the period of the blow in which the fluid flows in one direction and the total cycle period.

$$\tau = \frac{\psi}{f} \quad (10)$$

In an ideal regenerator, the effectiveness is a function of the NTU and the utilization factor. Therefore, in this work the experimental tests are carried out by varying the NTU while maintaining the utilization factor fixed.

3.2 PRESSURE DROP

To design the hydraulic system in a proper way, it is crucial to know the pressure drop along all the components of the magnetocaloric refrigeration device, including the AMR. Otherwise, the hydraulic pump may either not be able to provide the mass flow rate required to operate in an optimized condition or be oversized, thus operating far from the mass flow rate range where it is efficient, resulting in a higher energy consumption. Another effect of an oversized pump is the necessity of bigger heat transfer area (or bigger fans) to reject the heat to the external ambient as the friction losses result in the heating of the fluid (Nakashima *et al.*, 2021).

Therefore, the pressure drop is evaluated separately in the cold and hot blows (Eqs. 11 and 12) by using four pressure transducers, one pair for the cold blow ($P_{C,\text{out}}$ and $P_{H,\text{in}}$) and another for the hot blow ($P_{H,\text{out}}$ and $P_{C,\text{in}}$) as shown in the schematic diagram (Fig.2).

$$\Delta P_{\text{cb}} = P_{C,\text{out}} - P_{H,\text{in}} \quad (11)$$

$$\Delta P_{\text{hb}} = P_{H,\text{out}} - P_{C,\text{in}} \quad (12)$$

Looking at the schematic diagram, there are two available pairs of pressure transducers to obtain the pressure drop for each blow (cold or hot). For instance, in the cold blow, instead of choosing the pair $P_{C,\text{out}}$ and $P_{H,\text{in}}$, it is possible to use the pair $P_{C,\text{in}}$ and $P_{H,\text{out}}$. However, there is no fluid flowing in the former (in contrast with the latter), thus, there is no pressure drop between the pressure transducer and the regenerator inlet, which makes possible to isolate the pressure drop through the regenerator without considering the tubing.

With the pressure drop results and the corresponding mass flow rate, the Reynolds number and friction factor of each test was obtained, respectively with Eq. (13) (Kaviany, 1995; Trevizoli, 2015) and Eq. (14).

$$f_D = \frac{\epsilon^3}{1 - \epsilon} \frac{d_p}{\rho_f u^2} \frac{\Delta P}{L_{\text{reg}}} \quad (13)$$

$$Re_{dp} = \frac{\rho_f v d_p}{\mu} \quad (14)$$

where ρ_f is the fluid density, μ is the fluid viscosity, ΔP is the pressure drop through the regenerator, v is the superficial flow velocity and L_{reg} is the regenerator length. The experimental results obtained were compared to the numerical ones, in which the pressure drop is evaluated with the Eq. (15) (Irmay, 1958; Nield and Bejan, 2006).

$$\frac{dP}{dx} = - \frac{\beta \mu (1 - \epsilon)^2 v}{d_p^2 \epsilon^3} - \frac{\alpha \rho_f (1 - \epsilon) v^2}{d_p \epsilon^3} \quad (15)$$

where α and β are shape factors that must be determined empirically for each matrix. With $\alpha = 1.75$ and $\beta = 150$ this is equivalent to Ergun's Equation. This equation will be used to compare the obtained experimental results with a monodispersed packed bed of spheres, where the equation can be properly applied.

Ideally, one test would be sufficient to characterize the pressure drop within the regenerator in both directions. However, as mentioned before, La-Fe-Si alloys are usually brittle, therefore, the tests were carried out regularly to check the integrity of the solid matrix as the pressure drop usually increases when the materials that compose the regenerator start presenting mechanical failures.

4. RESULTS

This section is dedicated to presenting the results of the experimental evaluation of the regenerator. Initially, the heat transfer characterization will be presented followed by the hydraulic characterization as well as the evaluation of the mechanical stability. It is important to mention that all of the heat transfer characterization tests were carried out twice in order to reduce the uncertainties of the results.

4.1 EFFECTIVENESS RESULTS

In order to maintain the utilization fixed while the NTU is changed, as presented before in Section 3, the blow fraction, frequency and mass flow rate were varied. The selected blow fractions were 37,5% and 50%, the mass flow rates ranged from 40 to 100 kg/h and the frequency ranged from 0.25 to 0.9 Hz. The hot reservoir temperature was kept at 28 °C and the temperature span across the regenerator was kept fixed at 20 °C in order to reduce the influence of the thermocouples uncertainty (0.2 °C). These values were chosen in order to operate the regenerator with the utilization factor varying from 0.41 to 0.8, which is, in most cases, within the range for the optimal operation of the AMR (from 0.2 to 0.8) (Kitanovski *et al.*, 2015). Even though the tests are carried out under no magnetic field, the regenerator characterization is performed in the same range it is expected to operate during active testing, i.e., tests carried out in the regenerator under a changing applied magnetic field to evaluate the AMR cooling capacity.

To ensure that the regenerator is operating at steady state conditions, the acquisition of data starts a few minutes after setting the experimental condition parameters. Typical temperature and pressure drop profiles in an effectiveness characterization are shown in Fig. 4.

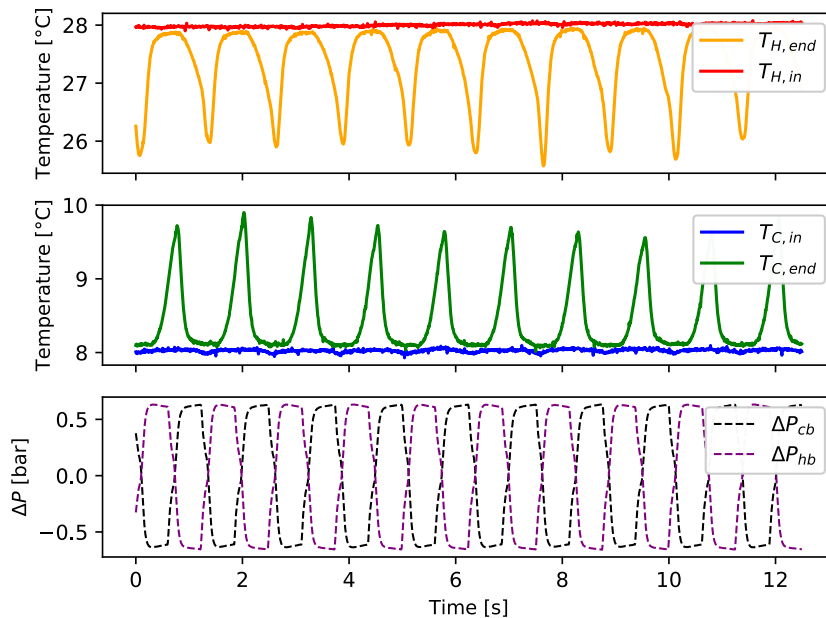


Figure 4: Temperature and pressure drop profiles as a function of time during several AMR cycles. The frequency was 0,8 Hz, the blow fraction (ψ) was 37,5% and the mass flow rate (\dot{m}) was 80 kg/h.

The pressure drop indicates when the regenerator is under hot or cold blow conditions, i.e, positive values of ΔP_{cb} occur when the fluid flow from the cold side to the hot side. On the other hand, the value of ΔP_{hb} is positive during the hot blow. Besides, there is an agreement between the pressure drop and temperature profile, namely, when the cold blow starts, the temperature of the cold side of the regenerator ($T_{C,end}$) approaches the cold reservoir temperature and,

at the same time, the temperature at the hot side of the regenerator ($T_{H,end}$) starts to decrease until the hot blow starts. Conversely, when the hot blow starts, the temperature of the hot side of regenerator ($T_{H,end}$) approaches the hot reservoir temperature and the temperature at the cold side of the regenerator ($T_{C,end}$) starts to increase until the hot blow finishes, initiating another cycle.

The effectiveness results for the experimental tests of the regenerator during the cold blow as a function of NTU and utilization are shown in Fig.5, where they are compared to the numerical results, which were obtained from the numerical model detailed by Vieira *et al.* (2021). The propagated uncertainty in the effectiveness results are estimated at 0.01. Analysing the results, some remarks can be made: 1) The effectiveness values achieved by this regenerator are all above 95%, what makes it suitable to be used as an AMR in a magnetic refrigeration device; 2) As the NTU increases, the effectiveness also tends also to increase as expected but, since it has almost reached the maximum possible value (1), the variations are subtle and, in some cases, are even within the uncertainty range; 3) There is a good agreement between the experiments and the model, which, in most cases, predicts the results within the uncertainty range. However, some of the numerical results overestimate the effectiveness over the uncertainty range. This can be explained due to the fact that the effectiveness was obtained assuming balanced flow, which is an idealization. In fact, the tests were carried out under slightly unbalanced flow conditions (normally under 1% in terms of difference in displaced mass during the hot and cold blow periods), which almost certainly had an impact on the effectiveness results.

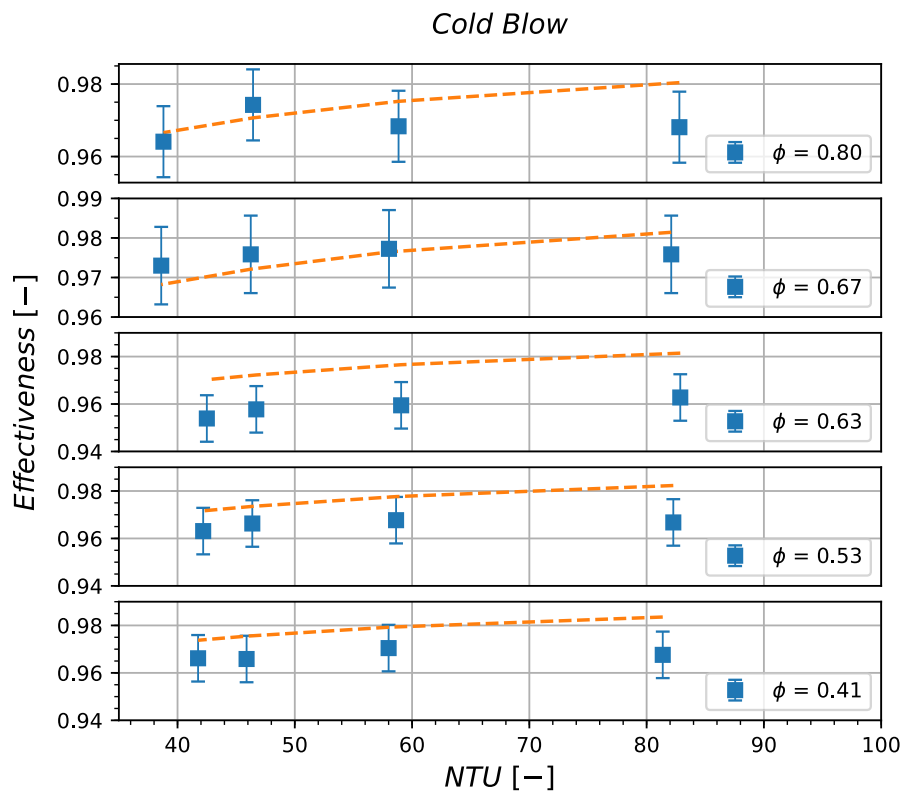


Figure 5: Comparison between the experimental and numerical results for effectiveness. Numerical results are represented by dashed lines while experimental results are represented by squares

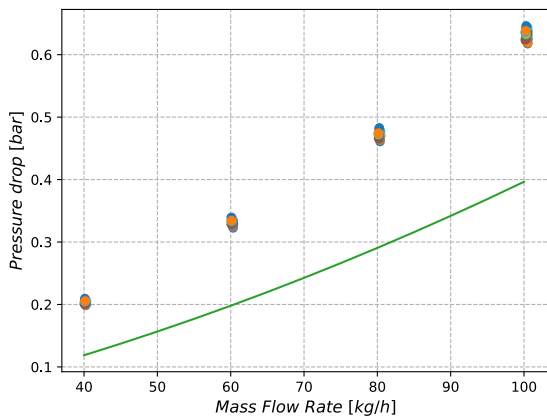
4.2 PRESSURE DROP AND MECHANICAL INTEGRITY

To experimentally characterize the pressure drop of the regenerator, the mass flow rate was varied from 40 to 100 kg/h in steps of 20 kg/h and the temperature of the fluid was kept at 25 °C. As mentioned before, these tests were performed both to evaluate the fluid flow resistance through the regenerator as well as its integrity, therefore, the tests were repeated several times at different days under the same experimental conditions.

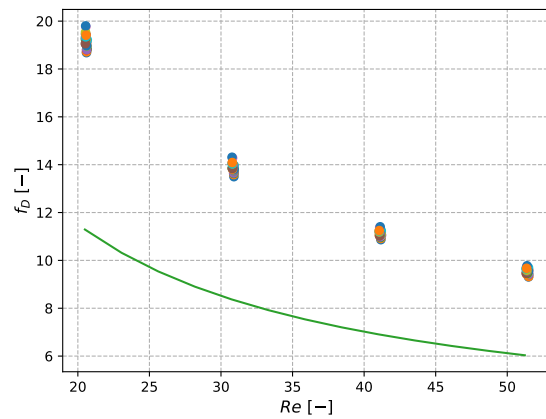
Figure 7 shows both the experimental and numerical results obtained with Ergun's equation, and it is possible to see that the experimental results (markers) presented a higher pressure drop when compared to the numerical ones (solid green line). This is probably due to the assumption of identical (same size) spherical particles in the numerical model, since the particles that compose the regenerator are fairly irregular (Fig. 6) as a result of its extrusion during the manufacturing process. The fixed particle diameter assumption in the model can also be responsible for the result as it ignores the distribution by setting an average value, but further investigations are needed to confirm this hypothesis.



Figure 6: Regenerator particles.



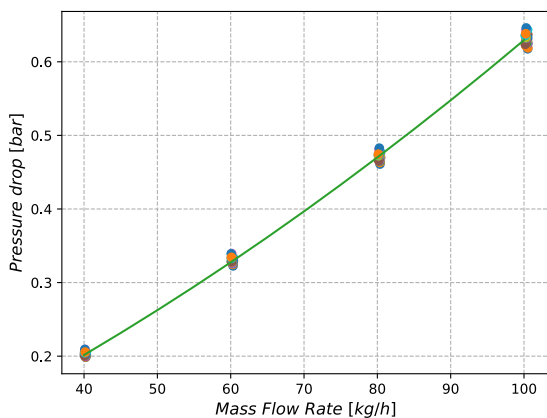
(a) Pressure drop as a function of the mass flow rate.



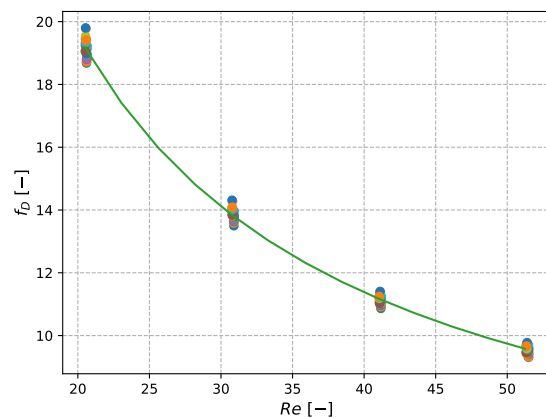
(b) Friction factor as function of the Reynolds number.

Figure 7: Pressure drop and friction factor experimental results compared with the Ergun's equation

Therefore, in order to calibrate the model to the present solid matrix, the shape factors α and β (Eq. 15) were determined by the least squares method and the results are shown in Fig. 8, where the values for α and β are, respectively 3.26 and 620.



(a) Pressure drop as a function of the mass flow rate.



(b) Friction factor as function of the Reynolds number.

Figure 8: Pressure drop and friction factor results. Adjusted shape factors.

To check the mechanical integrity of the regenerator, cumulative pressure drop variation (the ratio of the pressure drop in each day to the first day value) was analyzed and the results are shown in Fig. 9.

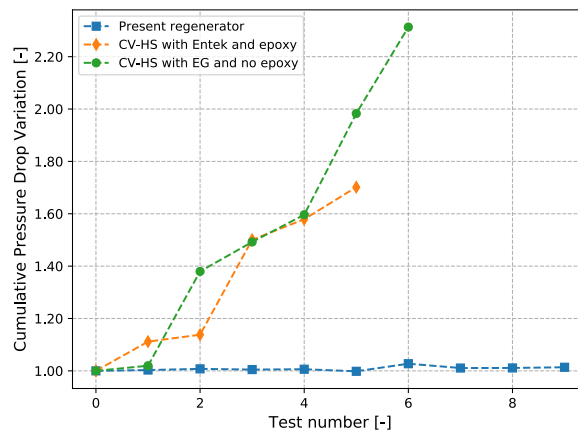


Figure 9: Cumulative pressure drop variation.

Figure 9 shows the experimental results of the pressure drop throughout the days of testing (each test number corresponds to a day of testing) for 3 regenerators, which were assembled using slightly different material compositions and operated with different working fluids. The regenerator characterized in this work is identified as "Present regenerator" and it used a 2 vol% Entek-water solution as the working fluid to prevent corrosion just like in the regenerator identified as "CV-HS with Entek and epoxy". The tests of the regenerator identified as "CV-HS with EG and no epoxy" were carried out with a 20 vol% ethylene glycol-water solution (EG) also for corrosion prevention purposes. Besides, the MCM of the "Present regenerator" has a different composition than the other two (higher alpha-iron concentration) and no epoxy is used as a binding agent like in the regenerator identified as "CV-HS with EG and no epoxy", while regenerator "CV-HS with Entek and epoxy" uses epoxy.

When compared to the results of the other two regenerators, the "Present regenerator" doesn't seem to present any mechanical stability issues as its pressure drop after being characterized remains almost constant after several days of testing. In contrast, the other regenerators, which have broken, presented a large increase in pressure drop already in the first days of testing. Therefore this regenerator seems to have better mechanical stability when compared with previous experimentally tested regenerators, which indicates it may be suitable for magnetic refrigeration applications.

5. CONCLUSIONS

A regenerator composed of a magnetocaloric material was assembled and characterized in terms of its thermo-hydraulic performance, namely the effectiveness as a function of NTU and friction factor as a function of Reynolds number. Afterwards, the experimental results were compared to simulations results in order to calibrate and validate the model.

The results showed that the regenerator presented high values of effectiveness (all above 95 %) what makes it suitable for magnetic refrigeration applications. In addition, it was observed a good agreement between the experiments and the simulations results. The friction factor results were compared to the Erguns's Equation and it was noticed that the hypothesis of a monodispersed packed bed of spheres was not suitable to the present regenerator. Therefore, shape factors were empirically determined in order to calibrate the model.

Besides that, the regenerator seems to be mechanically stable as its pressure drop shows no increases throughout the tests. However, despite the satisfactory results, it is important to continue testing for more time and under magnetization and demagnetization cycles, which introduce new loads in the material, to verify if it keeps its stability since the regenerator must withstand a lot more cycles than those which it has been able to resist in order to operate in a commercial magnetic refrigeration device.

6. ACKNOWLEDGEMENTS

Financial support from CNPq, CAPES, CODEMGE and the EMBRAPII Unit Polo/UFSC is duly acknowledged

7. REFERENCES

- Engelbrecht, K., 2008. *A numerical model of an active magnetic regenerator refrigerator with experimental validation*. Ph.D. thesis, University of Wisconsin-Madison.
- Hausen, H., 1983. *Heat Transfer in Counterflow, Parallel-Flow and Cross-Flow*. McGraw-Hill Co.,
- Irmay, S., 1958. "On the theoretical derivation of darcy and forchheimer formulas." *Eos, Trans. AGU*, Vol. 39, p. 702–707.
- Kaviany, M., 1995. *Principles of Heat Transfer in Porous Media*. 2. ed [S.1]. Springer.

- Kitanovski, A., 2020. “Energy applications of magnetocaloric materials”. *Advanced Energy Materials*.
- Kitanovski, A., Tušek, J., Tomc, U., Plaznik, U., Ožbolt, M. and Poredoš, A., 2015. *Magnetocaloric Energy Conversion: From Theory to Applications*. Springer.
- Lei, T., Navickaite, K., Engelbrecht, K., Barcza, A., Vieyra, H., Nielsen, K.K. and Bahl, C.R.H., 2018. “Passive characterization and active testing of epoxy bonded regenerators for room temperature magnetic refrigeration”. *Applied Thermal Engineering*, Vol. 128, pp. 10–19.
- Liang, J., Nielsen, K.K., Engelbrecht, K. and Bahl, C.R.H., 2020. “Heat transfer figures of merit for mapping passive regenerator performance to active regenerator cooling power”. *Applied Thermal Engineering*, Vol. 181.
- Lionte, S., Barcza, A., Risser, M., Muller, C. and Katter, M., 2021. “Lafesi-based magnetocaloric material analysis: Cyclic endurance and thermal performance results”. *International Journal of Refrigeration*, Vol. 124, pp. 43–51.
- Nakashima, A.T.D., Fortkamp, F.P., de Sá, N.M., dos Santos, V.M.A., Hoffmann, G., Peixer, G.F., Dutra, S.L., Ribeiro, M.C., Lozano, J.A. and Barbosa, J.R., 2021. “A magnetic wine cooler prototype”. *International Journal of Refrigeration*, Vol. 122, pp. 110–121.
- Nellis, G. and Klein, S., 2009. *Heat Transfer*. S.1. Cambridge University Press.
- Nield, D.A. and Bejan, A., 2006. *Convection in Porous Media*. 3a. ed [S.l.:s.n.]. Springer International Publishing.
- Pallares, J. and Grau, F.X., 2010. “A modification of a nusselt number correlation for forced convection in porous media”. *International Communications in Heat and Mass Transfer*, Vol. 37, pp. 1187–1190.
- Rowe, A., Tura, A., Dikeos, J. and Chahine, R., 2005. “Near room temperature magnetic refrigeration”. *Proceedings of the International Green Energy Conference*.
- Smith, A., Bahl, C.R.H., Bjørk, R., Engelbrecht, K., Nielsen, K.K. and Pryds, N., 2012. “Materials challenges for high performance magnetocaloric refrigeration devices”. *Advanced Energy Materials*, Vol. 2, pp. 1288–1318,.
- Trevizoli, P.V., 2015. *Development of thermal regenerators for magnetic cooling applications*. Ph.D. thesis, Federal University of Santa Catarina, Florianópolis, Brasil.
- Trevizoli, P.V. and Barbosa, J.R., 2020. “Overview on magnetic refrigeration”. In *Reference Module in Materials Science and Materials Engineering*, Elsevier.
- Vieira, B.P., Bez, H.N., Kuepferling, M., Rosa, M.A., Schafer, D., Cid, C.C.P., Vieyra, H.A., Basso, V., Lozano, J.A. and Barbosa, J.R., 2021. “Magnetocaloric properties of spheroidal $\text{La}(\text{Fe,Mn,Si})_{13}\text{H}_y$ granules and their performance in epoxy-bonded active magnetic regenerators”. *Applied Thermal Engineering*, Vol. 183.

8. RESPONSIBILITY NOTICE

The authors are solely responsible for the printed material included in this paper.